Stability and electronic properties of vacancies and antisites in BC_2N nanotubes

J. Rossato and R. J. Baierle*
Departamento de Física, Universidade Federal de Santa Maria, 97105-900 Santa Maria, Rio Grande do Sul, Brazil

W. Orellana
Departamento de Ciencias Físicas, Universidad Andrés Bello, Av. República 252, 837-0134 Santiago, Chile
(Received 27 September 2006; revised manuscript received 28 December 2006; published 1 June 2007)

The equilibrium geometry, energetic, and electronic properties of antisites and vacancies in BC_2N nanotubes are studied by spin density-functional calculations. We investigate these defects in both the zigzag (4,0) and the armchair (3,3) nanotubes. We find that boron and nitrogen, occupying nonequivalent carbon sites (B_{CII} and N_{CI}) in both tubes, have the lowest formation energies, showing that they are energetically favorable to form under B-rich and N-rich growth conditions. They also exhibit acceptor and donor properties, suggesting the formation of defect-induced *p*-type and *n*-type BC_2N nanotubes. In addition, carbon at boron and nitrogen sites (C_B and C_N) also exhibit *p*-type and *n*-type properties, respectively, as well as low formation energies. Vacancies are less favorable defects with high formation energies as compared to the most stable antisites. Once a vacancy is formed, a strong reconstruction occurs, resulting in an undercoordinated atom which typically gives rise to deep levels in the band gap, changing the electronic properties of the nanotube. Our results suggest that with suitable growth conditions, it would be possible to synthesize BC_2N nanotubes with intrinsic donor and acceptor character by inducing selective antisite defects.

DOI: 10.1103/PhysRevB.75.235401 PACS number(s): 71.15.Nc, 73.63.Fg, 73.22.−f, 71.55.−i

I. INTRODUCTION

The structural similarity between graphite and boron nitride graphitic compound coupled with the fact that both materials can form tubular structures has suggested the existence of intermediate ternary compound $B_xC_yN_z$ nanotubes.[1] These nanotubes were predicted by calculations[1–4] and recently synthesized using different methods such as chemical-vapor deposition,[5–7] arc discharge,[8–10] and pyrolysis.[11] A review on growth methods of BCN nanotubes can be found in Ref. 12. It is believed that their stability and electronic properties can vary between the homogeneity of carbon nanotubes (CNTs) and the heterogeneity of boron nitride nanotubes (BNNTs), depending on the stoichiometry. First-principles calculations have shown that CNTs can be metallic or semiconducting, depending on the tube diameter and chirality.[13] However, similar calculations show that all BNNTs are semiconducting with an almost fix energy gap of about 5.5 eV, independent of the geometry.[14] The above results suggest that the electronic properties of BCN nanotubes could be controlled by suitable variations in their stoichiometry, resulting attractive as an electronic device material.

For the hexagonal compound $B_xC_yN_z$ structure, the BC_2N stoichiometry is believed to be the most stable. Three stable ternary nanotubes obtained by rolling the hexagonal BC_2N sheet are known, which are labeled as types I, II, and III.[15] Theoretical results by Miyamoto *et al.*[1] have shown that (2,2) BC_2N nanotubes of type I are metallic, whereas those of type II are semiconducting. In that work, it is also suggested that the electronic properties of type-I nanotubes are expected to be similar to those of the carbon ones, i.e., metal or semiconductor, depending on their diameter and chirality. On the other hand, type-II nanotubes are expected to be semiconductors like the BN ones. Concerning the stability, the type-II structure optimizes the bond energy by maximizing the number of C-C and B-N bonds, which are stronger than the bonds resulting from other combinations of B, C, and N atoms. This would explain the higher stability obtained by *ab initio* calculations for the type-II structure as compared to types I and III.

Recently, calculations in BCN compound nanotubes have shown that these nanostructures are very promising for energy-storage applications due to their superior lithium adsorption capability,[16] as well as for nanotube-based molecular sensors.[17] These calculations were performed considering pristine nanotubes. However, an important point not yet elucidated in this kind of tube is the role played by defects, such as antisites (an atom occupying the site of another one) and vacancies (the absence of an atom). These defects may be present in the samples or may be induced by irradiation in the case of vacancies. According to tight-binding calculations, BC_2N nanotubes containing antisites such as carbon in a boron site (C_B) and carbon in a nitrogen site (C_N), are found to give rise to shallow levels in the nanotube band gap, showing *p*-type and *n*-type characters, respectively.[1] However, other antisites, such as N_C and B_C, are expected to have similar electronic properties. Thus, it is important to explore the stability of different defects in ternary nanotubes to have an entire picture about their possible use as electronic materials. In this work, we investigate the energetic and electronic properties of all vacancies and antisites in BC_2N nanotubes by first-principles calculations.

II. THEORETICAL METHOD

The calculations were carried out in the framework of the spin density-functional theory, with the generalized gradient approximation to the exchange-correlation functional.[18] We use a basis set consisting of strictly localized numerical pseudoatomic orbitals, as implemented in the SIESTA code,[19] namely, double-ζ (DZ) basis set. Norm-conserving

pseudopotentials[20] in their fully separable form[21] are used to describe the electron-ion interaction. Vacancy and antisite defects are studied in type-II BC_2N nanotubes, the zigzag (4,0) and the armchair (3,3), which have 6.54 and 8.34 Å in diameter, respectively. Both (3,3) and (4.0) tubes were described with supercells containing two basic BC_2N unit cells, containing 96 and 128 atoms, respectively, where periodic boundary conditions are applied along the tube axis. We consider one defect per supercell, which means we are calculating an infinite nanotube with linear density of defects. Thus, the densities of defects in (3,3) and (4,0) nanotubes are approximately of 0.06 and 0.07 defect/Å, respectively.

For the Brillouin-zone (BZ) sampling, we use two special k points,[22] along the tube axis. We check the band structure and the equilibrium geometry for nitrogen occupying a carbon site (N_{CI}) in the (4,0) tube, a metallic system, considering six k points according to the Monkhorst-Pack mesh.[22] Our results do not show any significant variation in the structural and electronic properties with respect to the two k-point calculations. The variation in the total energy between both k samplings is found to be of 0.075 eV/cell. Similar results were obtained for the carbon vacancy, ensuring a good convergence for the BZ sampling with two k points. We also check the convergence of the DZ basis set against an extended basis containing single-polarized functions, namely, DZP. A comparison between DZ and DZP band-structure calculations shows a small decrease in the band gap, of about 0.06 eV, maintaining essentially the same characteristics, whereas variations in the equilibrium geometry are negligible. To ensure minimal interaction between tube images within the supercell approach, we consider a vacuum region of about 9 Å. The positions of all atoms in the defective nanotubes were relaxed using the conjugated gradient algorithm until the force components become smaller than 0.05 eV/Å. The equilibrium geometry of a vacancy is found by considering preestablished initial geometries and comparing their energies after relaxation.

The formation energies of the antisite (X_Y, the atom X at the Y atom site) and vacancies (V_X, the absence of the X atom) are determined according to the equations

$$E_{\text{form}}[X_Y] = E_t[NT + X_Y] - E_t[NT] - \mu_X + \mu_Y, \quad (1)$$

and

$$E_{\text{form}}[V_X] = E_t[NT + V_X] - E_t[NT] + \mu_X, \quad (2)$$

where E_{form} and E_t are the formation and total energies of the defective systems. $E_t[NT]$ is the total energy of the pristine nanotube. μ are the chemical potentials of the atomic species. In this work, the chemical potential (μ_B, μ_C and μ_N) are calculated as the total energy per atom of the bulk phase of boron (α-B) and graphite, as well as the N_2 molecule. Following previous calculations,[23–26] we consider the variation of chemical potentials as constrained by the thermodynamic equilibrium condition

$$\mu_N + \mu_B = \mu_{BN}, \quad (3)$$

where μ_{BN} is the chemical potential for a BN pair in hexagonal boron nitride (h-BN). Upper limits for μ_B and μ_N are the energy per atom of α-B and the N_2 molecule, respectively. Assuming that μ_B (μ_N) takes its upper limit in Eq. (3) results in a B-rich (N-rich) condition for the defect formation energies, as calculated in Eqs. (1) and (2). Considering these extreme conditions, we can simulate the most favorable environment where vacancies and antisites could be formed.

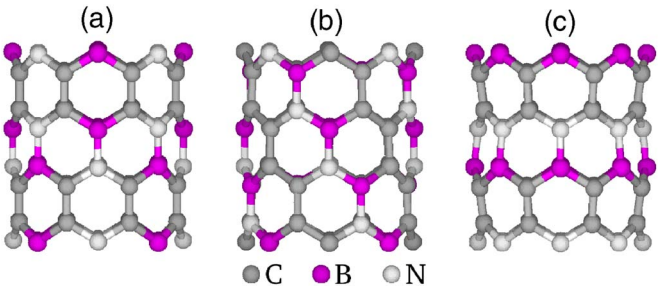

FIG. 1. (Color online) Equilibrium geometry of the (4,0) BC_2N nanotube in the three most stable structures. (a) Type I, (b) type II, and (c) type III.

III. RESULTS AND DISCUSSION

A. Pristine nanotubes

Figure 1 shows the equilibrium geometries of three stable zigzag nanotubes obtained from the BC_2N hexagonal sheet. Our calculation shows that the cohesive energy per BC_2N unit of the type-II nanotube is 1 eV lower in energy than those of types I and III, whereas types I and III have similar cohesive energies. This result is in close agreement with previous theoretical calculations, showing the same trend.[15] In BN nanotubes, calculations have suggested that zigzag and armchair tubes with similar radii have similar energies.[27,28] However, experiments have reported a preference for zigzag tubes against armchair ones.[29] We find that type-II BC_2N nanotubes with similar diameters do not show a significant energy preference between the zigzag and the armchair structure. For instance, the zigzag (5,0) nanotube of 8.10 Å in diameter has a cohesive energy of 7.03 eV/atom, whereas the armchair (3,3) nanotube of 8.34 Å in diameter has a cohesive energy of 7.04 eV/atom. The small energy difference between both tubes can be related to their similar curvatures. On the other hand, the cohesive energy of the BC_2N sheet is calculated to be of 7.14 eV, indicating that for nanotube of about 8 Å in diameter, the strain energy can be estimated in 0.1 eV. The stability of BC_2N nanotubes can be estimated by calculating their heat of formation, according to the equation

$$\Delta H_f = E_t[BC_2N] - \mu_{BN} - 2\mu_C. \quad (4)$$

Our results show that both the zigzag (4,0) and the armchair (3,3) nanotubes are metastable structures against the formation of h-BN and graphite with heats of formation of 1.85 and 1.55 eV, respectively.

Figure 2 shows the calculated band structure of perfect zigzag and armchair nanotubes. The zigzag (4,0) has a direct band gap of 0.92 eV at the Γ point, whereas the armchair (3,3) has direct band gap of 1.14 eV at a point about $0.6\overline{\Gamma X}$. In both nanotubes, the charge density of the valence-band maximum (VBM) is mainly localized at the C atoms, which

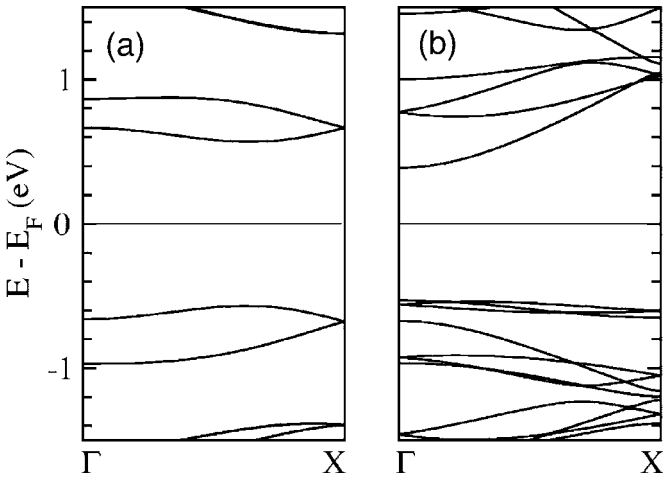

FIG. 2. Electronic band structures of type-II BC_2N nanotubes. (a) The armchair (3,3) nanotube. (b) The zigzag (4,0) nanotube.

have B and two C atoms as nearest neighbors (labeled as CI), whereas the charge density of the conduction-band minimum (CBM) is mainly localized at the C atoms, which have N and two C atoms as nearest neighbors (labeled as CII). The above results are in good agreement with previous *ab initio* calculations.[30,31]

B. Antisite defects

Antisites are probably the most common defects in ternary compound nanotubes, owing that they form far from the thermodynamic equilibrium. We study the energetic and electronic properties of the eight possible antisites in BC_2N nanotubes: boron in carbon sites (B_{CI} and B_{CII}), nitrogen in carbon sites (N_{CI} and N_{CII}), carbon in boron and nitrogen sites (C_B and C_N), boron in a nitrogen site (B_N), and nitrogen in a boron site (N_B). Our results for the formation energies of these antisites under both B-rich and N-rich growth conditions are summarized in Table I. Among all the antisites under study, B_C and N_C present the lower formation energies in both nanotubes, particularly B_{CII} (B rich) and N_{CI} (N rich) which exhibit negative values, showing higher stability than the pristine nanotubes. The lower formation energy observed for B_{CII} and N_{CI} in both nanotubes can be associated with the formation of new B-N bonds, whereas for B_{CI} and N_{CII} antisites, which have higher formation energies, new B-B and N-N bonds are created. The negative formation energies for the B_{CII} and N_{CI} also indicate that additional stable phases for the BC_2N nanotubes can occur, as recently suggested by *ab initio* calculations.[24,32]

TABLE I. Formation energies for antisite defects in zigzag (4,0) and armchair (3,3) BC_2N nanotubes calculated under boron rich (B-rich) and nitrogen rich (N-rich) growth conditions.

	E_{form} (eV)			
	(4,0)		(3,3)	
Antisite	B rich	N rich	B rich	N rich
B_{CI}	1.10	4.33	1.28	4.51
B_{CII}	−0.23	3.00	−0.31	2.92
N_{CI}	2.73	−0.50	3.06	−0.17
N_{CII}	4.24	1.01	4.46	1.23
C_B	2.95	−0.28	3.24	0.01
C_N	−0.07	3.16	−0.08	3.14
B_N	1.52	7.99	2.12	8.58
N_B	7.81	1.35	7.97	1.50

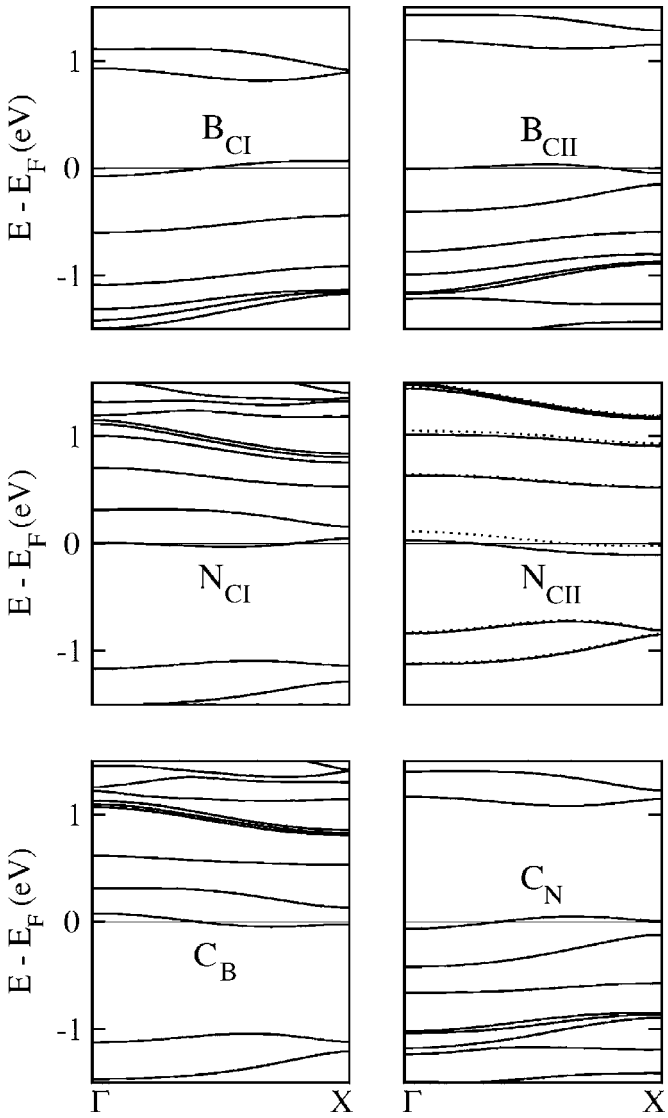

FIG. 3. Electronic band structures for the most stable antisites in the (3,3) armchair BC_2N nanotube. The continuous and dotted lines indicate majority and minority spin bands, respectively.

Figures 3 and 4 show the electronic band structures of six lower-energy antisites in BCN nanotubes. The energetically favorable antisites in (3,3) and (4,0) tubes (B_{CII} and N_{CI}, respectively) give rise to energy levels close to the band-gap edges, suggesting shallowlike defects with acceptor and donor characters, respectively. We note that the dispersion observed in these levels along ΓX is due to the high concentration of defects in the nanotubes. The highest-occupied level

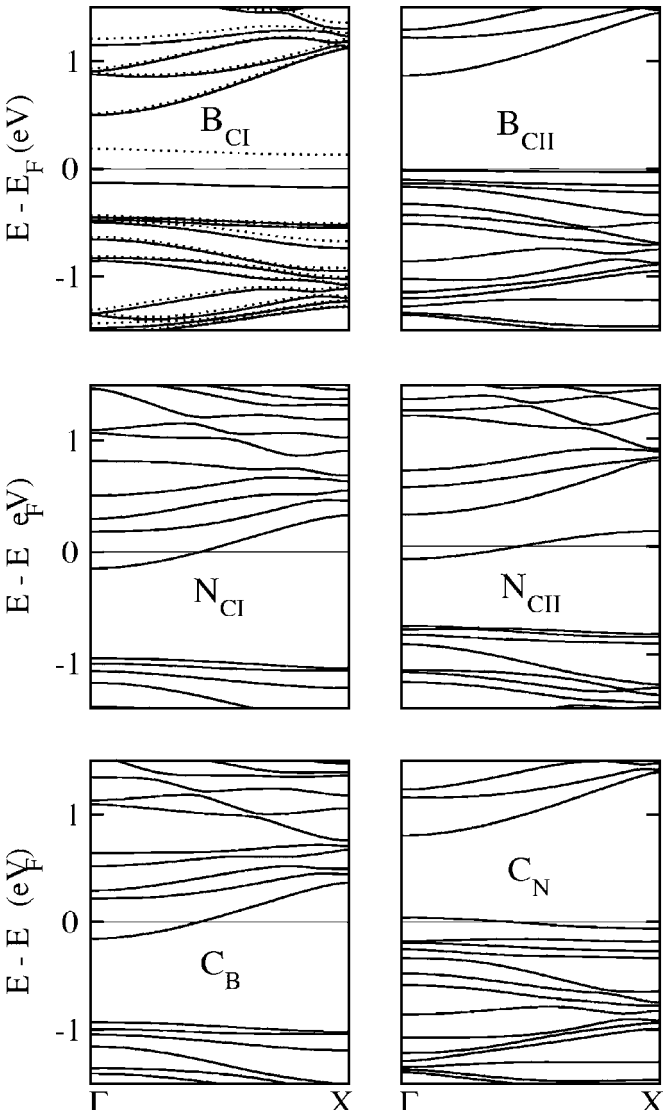

FIG. 4. Electronic band structures for the most stable antisites in the (4,0) zigzag BC_2N nanotube.

for B_{CII} in the (3,3) tube (top of the valence band) shows a dispersion of about 0.1 eV. Whereas for N_{CI} in the (4,0) tube (bottom of the conduction band), the dispersion is found to be about 0.5 eV. In nanotubes with more dilute defect concentration, the dispersions should decrease giving flat defect states. To check this, we calculate N_{CI} in the (4,0) tube doubling the supercell size along the tube axis, i.e., considering a concentration of about 0.03 defects/Å. Our results show that the dispersion of the highest-occupied level decreases up to 0.1 eV.

We note that antisites B_{CII} and C_N, and N_{CI} and C_B in both armchair and zigzag tubes show the same electronic properties, characterizing acceptor and donor defects, respectively, whereas other antisites give rise to defect levels deeper inside the band gap. According to our results, the appearance of shallowlike levels would depend on two conditions: (i) the difference in valence between the guest defect and the host site might be one, and (ii) one of the three bonds of an antisite might be C-C or B-N. The latter would be also a requirement to the most stable antisites.

TABLE II. Formation energies for vacancies defects in zigzag (4,0) and armchair (3,3) BC_2N nanotubes.

	E_{form} (eV)			
	(4,0)		(3,3)	
Vacancy	B rich	N rich	B rich	N rich
V_{CI}	4.25	4.25	4.48	4.48
V_{CII}	5.19	5.19	4.95	4.95
V_B	6.32	3.09	6.37	3.14
V_N	2.75	5.98	3.70	6.93

Our results for the band structures of B_N and N_B antisites in both nanotubes show dispersionless deep levels in the band gap, indicating highly localized defect states. These antisites do not change the semiconducting character of the nanotubes, similarly to B_{CI} in the (4,0) nanotube (see Fig. 4). This different electronic behavior can be understood by the formation of B-B and N-N bonds between the antisite and their nearest neighbors, similar to those found in BN layer structures. In fact, theoretical results of antisites in BN nanotubes[25,26] show that B_N (N_B) have higher formation energies, rising deep levels in the band gap, whereas charge density associated with these levels is mainly localized at B-B (N-N) bonds, similar to those we have found in BC_2N nanotubes. It is interesting to note that relative deep levels are also found for B_{CI} and N_{CII} antisites in both nanotubes where B-B and N-N bonds are also formed, suggesting a trend for the deep-level appearance.

The possibility to create acceptor and donor levels induced by the antisites C_B and C_N in type-II (2,2) BC_2N nanotubes have already been investigated by Miyamoto *et al.*[1] using the tight-binding approach. The main electronic properties they report indicate an acceptorlike level (located 0.03 eV above the VBM) and a donorlike level (located 0.03 eV below the CBM) for C_N and C_B, respectively, showing that the C atom behaves as a shallow impurities at N and B sites in BC_2N nanotubes. Our calculations for the same antisites in the (3,3) tube agree qualitatively well with the above results, showing defect-induced levels close to the band edges. However, we find that C_N (C_B) is 0.23 eV (0.18 eV) higher in formation energy than B_{CII} (N_{CI}) under B-rich (N-rich) conditions. Therefore, our results suggest that the B_{CII} and N_{CI} would be energetically more favorable than C_N and C_B, showing similar acceptor and donor properties, respectively.

C. Vacancy defects

Vacancies in nanotubes are another defects which can be formed during synthesis processes or can be artificially induced by irradiation. Recently, the structural and electronic properties of vacancies in CNTs (Refs. 33–35) and in BNNTs (Refs. 25 and 26) have been investigated by *ab initio* calculations. When an atom is removed from those nanotubes, the neighboring atoms partially reconstruct around the defect,

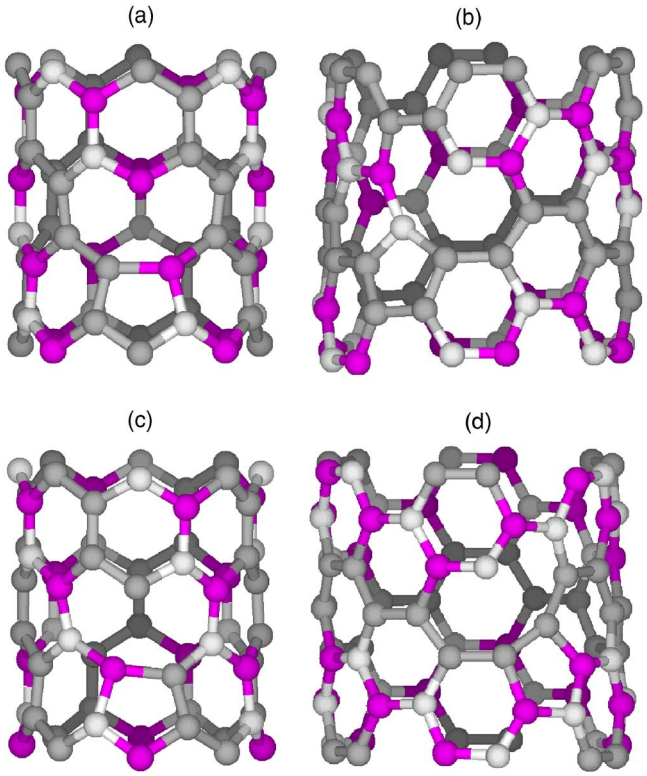

FIG. 5. (Color online) Equilibrium geometries for the most stable vacancies in BC_2N nanotubes. (a) V_N in the (4,0) tube, (b) V_B in the (3,3) tube, (c) V_{CI} in the (4,0) tube, and (d) V_{CII} in the (3,3) tube.

forming new five- and nine-membered rings. This results in an undercoordinated atom which moves slightly off the nanotube surface. The occupation of the dangling bond at the twofold-coordinated atom governs the electronic properties of the defective tube, which typically gives rise to deep levels in the nanotube band gap, altering their electronic properties.

We study the four possible vacancies in BC_2N nanotubes, namely, boron vacancy (V_B), nitrogen vacancy (V_N), and the vacancies of two nonequivalent carbon atoms (V_{CI} and V_{CII}). Table II shows our results for their formation energies. We find that V_N in the (4,0) tube and V_B in the (3,3) tube are the most stable ones under B-rich and N-rich conditions, with formation energies of 2.75 and 3.14 eV, respectively, whereas V_{CI} in the (4,0) tube and V_{CII} in the (3,3) tube have formation energies of 4.25 and 4.95 eV, respectively. The equilibrium geometries of the above vacancies are shown in Fig. 5. For V_N in the (4,0) tube, the twofold-coordinated atom is boron, which bind with a N and a C atom (hereafter the bonding structure N-B-C), whereas the new bond forming the pentagonal ring is B-C with a bond length of 1.65 Å [Fig. 5(a)]. For V_B in the (3,3) tube, the undercoordinated atom is nitrogen (B-N-C) and the bond that completes the pentagonal ring is N-C with a bond length of 1.52 Å [Fig. 5(b)]. We obtained the spin magnetic moment for the defective nanotubes, defined as $m_s=2S\mu_B$, where S is the total spin of the system and μ_B is the Bohr magneton. We find that V_N has a magnetic moment of $0.95\mu_B$, indicating that one electron occupies the dangling bond at the undercoordinated atom. Similar result is obtained for V_B, which shows a magnetic moment of $0.98\mu_B$. Strictly speaking, $m_s=1\mu_B$ implies in an unpaired electron; however, spin polarization effects in

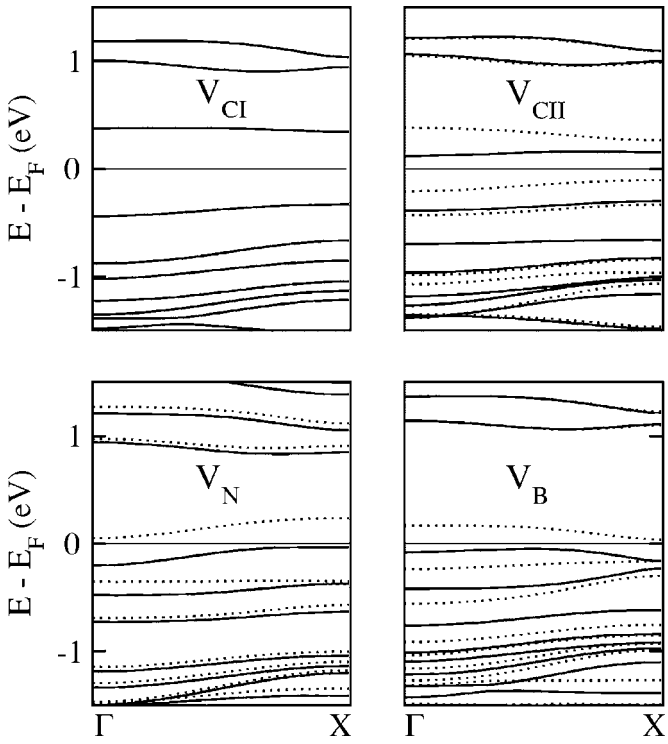

FIG. 6. Electronic band structures for vacancies in the (3,3) armchair BC_2N nanotube.

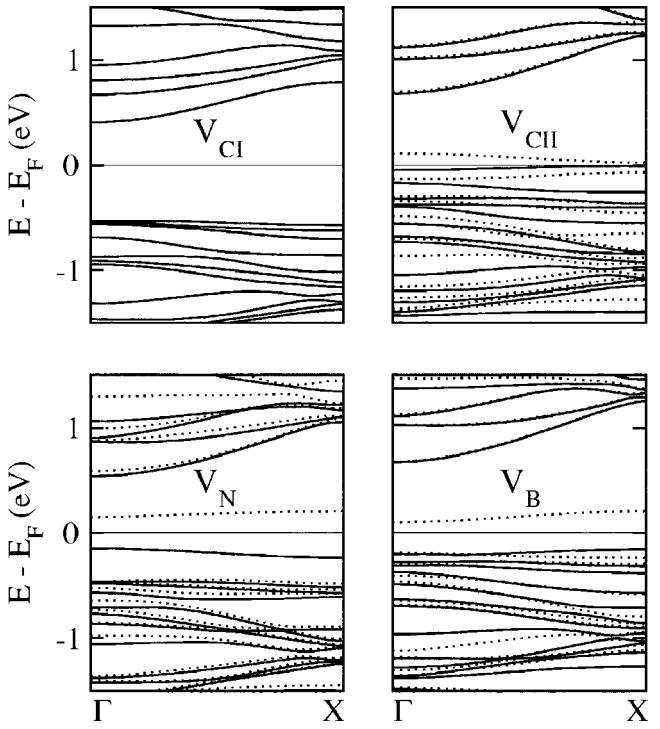

FIG. 7. Electronic band structures for vacancies in the (4,0) BC_2N nanotube.

the neighborhood of the dangling bond reduce the total magnetic moment.[34]

A different situation occurs for V_{CI} in both (3,3) and (4,0) tubes which show zero magnetic moments. Here, the undercoordinated atoms are nitrogen (B-N-C) and carbon (C-C-N) [Fig. 5(c)], respectively. In this case, no unpaired electron is found probably due to the formation of N-C double bonds. However, for V_{CII} in (3,3) and (4,0) tubes, the undercoordinated atoms are nitrogen (B-N-B) and carbon (B-C-C), and the magnetic moments are zero and $2\mu_B$, respectively. Therefore, for V_{CII} in the (4,0) tube, we find a high-spin configuration ($S=1$), originating in the two electrons that occupy the dangling bond, whereas for V_{CII} in the (3,3) tube, a low-spin configuration ($S=0$) for the unpaired electrons is observed.

Figures 6 and 7 show the band structure of the vacancies in the (3,3) and (4,0) tubes, respectively. We find that V_N and V_B in both tubes give rise to deep levels in the band gap, showing similar electronic characteristic. As these vacancies exhibit an unpaired electron in the dangling bond, the highest-occupied (spin up) and the lowest-empty (spin down) states correspond to the defect level after a spin-band splitting of about 0.3 eV. For the V_{CI} in the (4.0) tube (Fig. 7), no defect level in the band gap or spin-band splitting are observed. The above is consistent with the absence of electrons in the dangling bond at the undercoordinated atom. Compared with the band structure of the pristine tube [Fig. 2(b)], we can conclude that the major effect of V_{CI} in the (4.0) tube is a symmetry breaking. Similarly, the band structure of V_{CI} in the (3.3) tube (Fig. 6) does not show spin-band splitting. However, the difference in energy between the highest-occupied and lowest-empty subbands is about 0.4 eV lower in energy than that of the pristine tube [Fig. 2(a)]. This effect can also be associated with the symmetry breaking induced by the vacancy.

The band structure of V_{CII} in the (4,0) tube shows a semimetallic character, which could explain the high-spin configuration ($S=1$) for the two electrons occupying the dangling bond. However, for V_{CII} in the (3,3) tube, which also has two electrons at the dangling bond, a spin-band splitting is observed, which we believe is consistent with its semiconducting character and low-spin configuration ($S=0$).

IV. SUMMARY

In summary, we have studied the equilibrium geometry, energetic, and electronic properties of vacancies and antisites in the armchair (3,3) and the zigzag (4,0) BC_2N nanotubes, using spin-polarized density-functional calculations. We find that the most stable antisites B_{CII} and N_{CI} have negative formation energies under extreme B-rich and N-rich conditions, suggesting higher stabilities than pristine nanotubes. They also exhibit acceptor and donor properties, showing that *p*-type and *n*-type semiconductor BC_2N nanotubes would be favorable to form under these conditions. Similar characteristics show the carbon antisites C_N and C_B, which also have negative or close to zero formation energies under favorable conditions. On the other hand, antisites that form B-B bonds (B_{CI} and B_N) and N-N bonds (N_{CII} and N_B) have higher formation energies, giving rise to deeper levels in the nanotube band gap.

Concerning vacancies, we find that V_N in the (4,0) tube and V_B in the (3,3) tube are the most stable ones under B-rich and N-rich conditions, respectively. These vacancies show an unpaired electron in the dangling bond at the undercoordinated atom, giving rise to a single-occupied deep level in the band gap, which exhibits a spin-band splitting of about 0.3 eV. On the other hand, V_{CI} in both tubes do not show unpaired electrons at the undercoordinated atom due to the formation of double bonds, exhibiting electronic characteristic similar to the corresponding pristine nanotubes. However, a different situation occurs for V_{CII} where two electrons occupy the dangling bond in both tubes. In the (3,3) tube, the equilibrium structure shows $m_s=0$ and a semiconducting character, implying in a $S=0$ spin configuration, whereas in the (4,0) tube, it shows $m_s=2\mu_B$ and a semimetallic character, implying a $S=1$ spin configuration.

Finally, our results suggest that with suitable growth conditions, it would be possible to synthesize BC_2N nanotubes with intrinsic donor and acceptor character by inducing specific antisite defects. In addition, we find that the electronic properties of the nanotubes can change drastically by the presence of vacancies.

ACKNOWLEDGMENTS

This work was supported by the Brazilian agencies CNPq and CAPES. W. O. acknowledges financial support from Chilean agencies FONDECYT, under Grant No. 1050197, and the Millennium Nucleus of Applied Quantum Mechanics and Computational Chemistry, through Project No. P02-004-F. Most of the calculations were performed in the computational facilities of CENAPAD-SP.

*Electronic address: rbaierle@smail.ufsm.br

[1] Y. Miyamoto, A. Rubio, M. L. Cohen, and S. G. Louie, Phys. Rev. B **50**, 4976 (1994).
[2] X. Blase, J.-C. Charlier, A. De Vita, and R. Car, Appl. Phys. Lett. **70**, 197 (1997).
[3] X. Blase, J.-C. Charlier, A. De Vita, and R. Car, Appl. Phys. A: Mater. Sci. Process. **68**, 293 (1999).
[4] X. Blase, Comput. Mater. Sci. **17**, 107 (2000).
[5] X. D. Bai, J. Yu, S. Liu, and E. G. Wang, Chem. Phys. Lett. **325**, 485 (2000).
[6] J. Yu, X. D. Bai, J. Ahn, S. F. Yoon, and E. G. Wang, Chem. Phys. Lett. **323**, 529 (2000).
[7] L.-W. Yin, Y. Bando, D. Golberg, A. Gloter, M.-S. Li, X. Yuan, and T. Sekiguchi, J. Am. Chem. Soc. **127**, 16354 (2005).
[8] O. Stephan, P. M. Ajayan, C. Colliex, P. Redlich, J. M. Lambert, P. Bernier, and P. Lefin, Science **266**, 1683 (1994).
[9] Z. Weng-Sieh, K. Cherrey, N. G. Chopra, X. Blase, Y. Miyamoto, A. Rubio, M. L. Cohen, S. G. Louie, A. Zettl, and R. Gronsky, Phys. Rev. B **51**, 11229 (1995).
[10] P. Redlich, J. Loeffler, P. M. Ajayan, J. Bill, F. Aldinger, and M.

Ruhle, Chem. Phys. Lett. **260**, 465 (1996).
[11] S. Rahul, B. C. Satishkumar, A. Govindaraj, K. R. Harikumar, R. Gargi, J. P. Zhang, A. K. Cheetham and C. N. R. Rao, Chem. Phys. Lett. **287**, 671 (1998).
[12] M. Terrones, N. Grobert, and H. Terrones, Carbon **40**, 1665 (2002).
[13] R. Saito, G. Dresselhaus, and M. S. Dresselhaus, *Physical Properties of Carbon Nanotubes* (World Scientific, London, 1998).
[14] X. Blase, A. Rubio, S. G. Louie, and M. L. Cohen, Europhys. Lett. **28**, 335 (1994).
[15] A. Y. Liu, R. M. Wentzcovitch, and M. L. Cohen, Phys. Rev. B **39**, 1760 (1989).
[16] Z. Zhou, J. Zhao, X. Gao, Z. Chen, J. Yan, P. R. Schleyer, and M. Morinaga, Chem. Mater. **17**, 992 (2005).
[17] S. Peng and K. Cho, Nano Lett. **3**, 513 (2003).
[18] J. P. Perdew, K. Burke, and M. Ernzerhof, Phys. Rev. Lett. **77**, 3865 (1996).
[19] J. M. Soler, E. Artacho, J. D. Gale, A. García, J. Junquera, P. Ordejón, and D. Sánchez-Portal, J. Phys.: Condens. Matter **14**, 2745 (2002).
[20] N. Troullier and J. L. Martins, Phys. Rev. B **43**, 1993 (1991).
[21] L. Kleinman and D. M. Bylander, Phys. Rev. Lett. **48**, 1425 (1982).
[22] H. J. Monkhorst and J. D. Pack, Phys. Rev. B **13**, 5188 (1976).
[23] W. Orellana and H. Chacham, Appl. Phys. Lett. **74**, 2984 (1999).
[24] M. S. C. Mazzoni, R. W. Nunes, S. Azevedo, and H. Chacham, Phys. Rev. B **73**, 073108 (2006).
[25] T. M. Schmidt, R. J. Baierle, P. Piquini, and A. Fazzio, Phys. Rev. B **67**, 113407 (2003).
[26] P. Piquini, R. J. Baierle, T. M. Schmidt, and A. Fazzio, Nanotechnology **16**, 827 (2005).
[27] H. J. Xiang, J. Yang, J. G. Hou, and Q. Zhu, Phys. Rev. B **68**, 035427 (2003).
[28] E. Hernández, C. Goze, P. Bernier, and A. Rubio, Phys. Rev. Lett. **80**, 4502 (1998).
[29] R. S. Lee, J. Gavillet, M. Lamy de la Chapelle, A. Loiseau, J.-L. Cochon, D. Pigache, J. Thibault, and F. Willaime, Phys. Rev. B **64**, 121405(R) (2001).
[30] H. Pan, Y. P. Feng, and J. Lin, Phys. Rev. B **74**, 045409 (2006).
[31] H. Pan, Y. P. Feng, and J. Y. Lin, Phys. Rev. B **73**, 035420 (2006).
[32] S. Azevedo, Phys. Lett. A **351**, 109 (2006).
[33] J. Rossato, R. J. Baierle, A. Fazzio, and R. Mota, Nano Lett. **5**, 197 (2005).
[34] W. Orellana and P. Fuentealba, Surf. Sci. **600**, 4305 (2006).
[35] A. J. Lu and B. C. Pan, Phys. Rev. Lett. **92**, 105504 (2004).